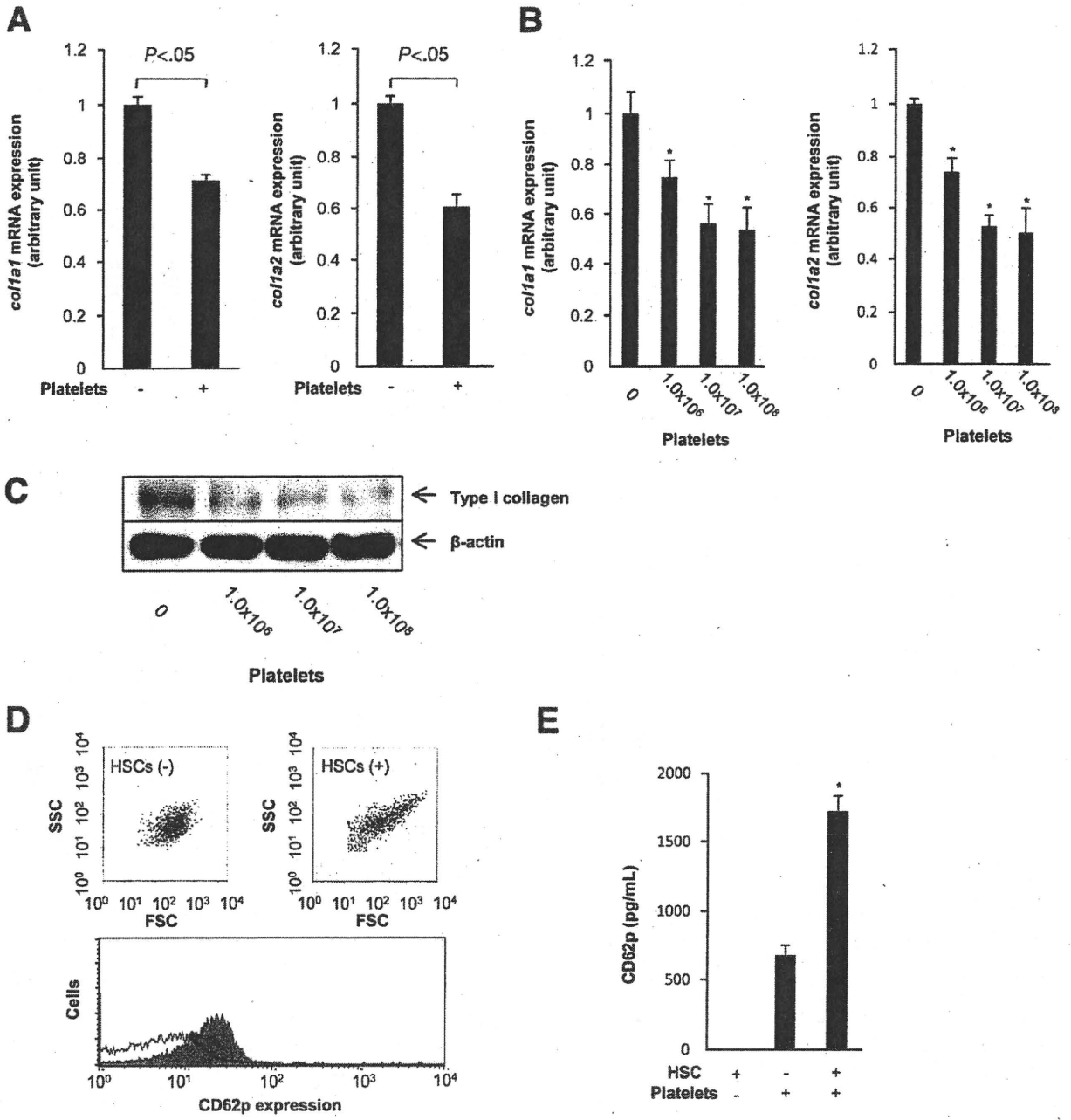

Figure 3. Platelets become activated and inhibit collagen synthesis in activated HSCs in vitro. (*A* and *B*) *col1a1* And *col1a2* mRNA levels in HSCs by real-time reverse-transcription polymerase chain reaction. Primary isolated HSCs were cocultured with 1.0×10^8 platelets for 6 hours (*A*), n = 3/group. HSCs (1.0×10^5) were cocultured with indicated dosages of platelets for 6 hours (*B*), n = 3/group, $^*P < .05$ vs HSCs with control group. (*C*) Expression of type I collagen protein in HSCs determined by Western blot analysis. HSCs (5.0×10^5) were cocultured with indicated dosages of platelets for 14 hours. (*D* and *E*) Activation of platelets on exposure to HSCs. Platelets (1.0×10^7) were cocultured with or without 1.0×10^5 HSCs for 1 hour. Shape change and P-selectin surface expression of platelets were analyzed by flow cytometry (*D*); representative data are shown; note that FSC increased with addition of HSCs; *closed histograms* and *open histograms* indicate P-selectin surface expression of platelets cocultured with or without HSCs, respectively. Soluble P-selectin levels of the culture supernatants were determined by ELISA (*E*), n = 3/group, $^*P < .05$ vs the other 2 groups.

HGF Administration Alleviates Liver Fibrosis in Thrombocytopenic Mice to the Level in the Control Littermates After BDL

To investigate the involvement of platelets in cholestasis-induced liver fibrosis in vivo, we examined platelet kinetics upon BDL treatment. To find whether platelets accumulate in the liver, we examined the expression of CD41 protein. Western blot analysis revealed that CD41 expression in the liver was up-regulated upon BDL treatment in the control littermates but not in the thrombocy-

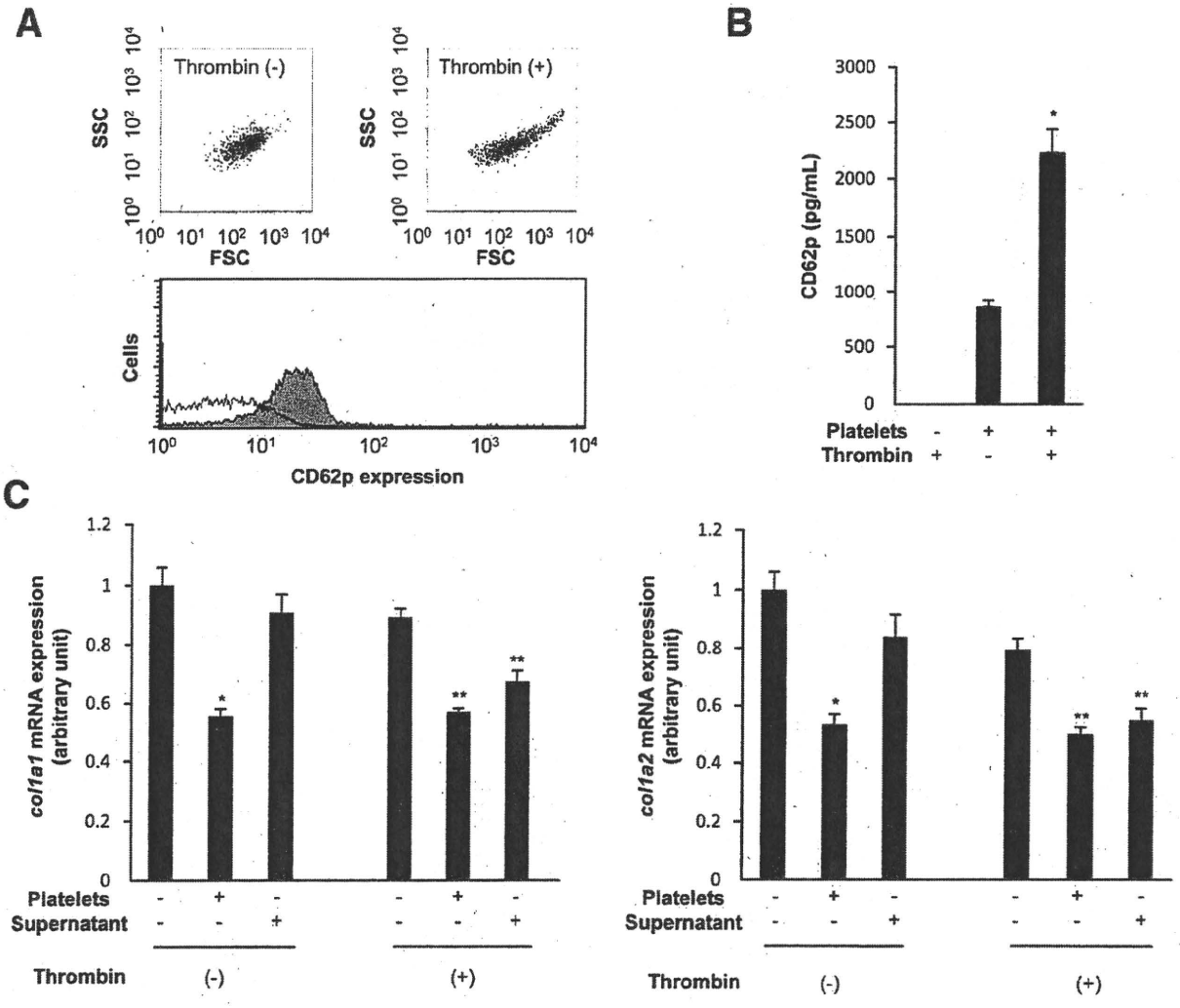

Figure 4. Soluble factors released from activated platelets are involved in the inhibition of collagen synthesis in HSCs. (*A* and *B*) Activation of platelets stimulated with thrombin. Platelets (1.0×10^7) were stimulated with or without thrombin (1 U/mL) for 15 minutes. Shape change and P-selectin surface expression of platelets were analyzed by flow cytometry (*A*); representative data are shown; note that FSC increased with addition of thrombin; *closed histograms* and *open histograms* indicate P-selectin surface expression of platelets stimulated with or without thrombin, respectively. Soluble P-selectin levels of the culture supernatants were determined by ELISA (*B*), n = 3/group, $^*P < .05$ vs the other 2 groups. (*C*) *col1a1* And *col1a2* mRNA levels in HSCs treated with the supernatant of activated or quiescent platelets by real-time reverse-transcription polymerase chain reaction. HSCs were cocultured with or without 1.0×10^7 platelets for 6 hours in the presence or absence of thrombin (1 U/mL). In parallel, HSCs were cultured for 6 hours with the supernatants of platelets, which had been stimulated with or without thrombin (1 U/mL) for 15 minutes, n = 3/group. $^*P < .05$ vs HSC with control group and HSC with platelet supernatant group. $^{**}P < .05$ vs HSC with thrombin group.

topenic mice (Figure 6*A*). Furthermore, phosphorylation of Met protein in the liver occurred upon BDL treatment, but it was weaker in the thrombocytopenic mice than in the control littermates (Figure 6*B*). Similar attenuation of Met phosphorylation in the thrombocytopenic mice was also observed at 3 days after BDL (Supplementary Figure 2). These results indicated that BDL-induced cholestasis led to intrahepatic platelet accumulation and activated the Met signal in the liver. In contrast, both were attenuated in the liver of the thrombocytopenic mice. Furthermore, plasma HGF levels in the thrombocytopenic mice did not increase upon BDL and were evidently lower than in the control littermates (Figure 6*C*). Finally, to investigate whether attenuation of Met activation in the liver of the thrombocytopenic mice was involved in the exacerbation of liver fibrosis, we tested the hypothesis that administration of HGF, known to exert an antifibrotic effect,[20-22] would alleviate liver fibrosis in the thrombocytopenic mice more than in the control littermates. These mice were treated with either vehicle or recombinant HGF following BDL. As expected, HGF administration alleviated liver fibrosis in the thrombocytopenic mice to the level found in the control littermates (Figure 6*D*). Notably, elevated hepatic expression of type I collagen genes in the thrombocytopenic mice was also attenuated to a level comparable with that in the control littermates by the HGF therapy (Figure 6*E*).

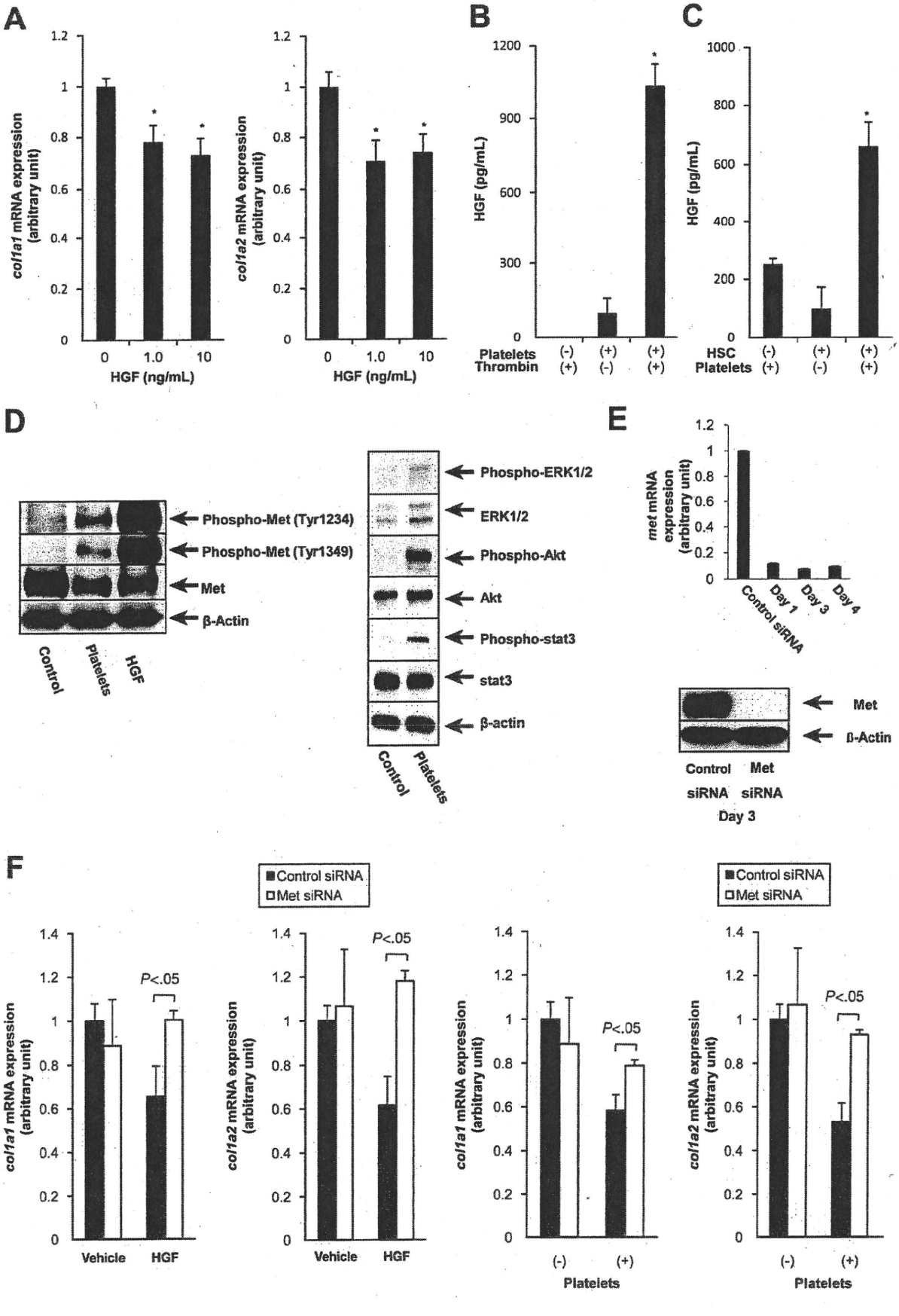
A
col1a1 mRNA expression (arbitrary unit)
HGF (ng/mL)
col1a2 mRNA expression (arbitrary unit)
HGF (ng/mL)
B
HGF (pg/mL)
Platelets
Thrombin
C
HGF (pg/mL)
HSC
Platelets
D
Phospho-Met (Tyr1234)
Phospho-Met (Tyr1349)
Met
β-Actin
Control
Platelets
HGF
Phospho-ERK1/2
ERK1/2
Phospho-Akt
Akt
Phospho-stat3
stat3
β-actin
Control
Platelets
E
met mRNA expression (arbitrary unit)
Control siRNA
Day 1
Day 3
Day 4
Met
β-Actin
Control siRNA
Met siRNA
Day 3
F
Control siRNA
Met siRNA
col1a1 mRNA expression (arbitrary unit)
P<.05
Vehicle
HGF
col1a2 mRNA expression (arbitrary unit)
P<.05
Vehicle
HGF
col1a1 mRNA expression (arbitrary unit)
P<.05
Platelets
col1a2 mRNA expression (arbitrary unit)
P<.05
Platelets

Discussion

Platelets are circulating blood cells with the daily job of handling hemostasis and thrombosis.[14] On the other hand, they are also involved in inflammation,[23] angiogenesis, and tissue repair. Platelets have been shown to accumulate in the liver under some pathologic conditions such as acute viral hepatitis[24] and cholestasis.[25] Previous work on such situations has focused on platelets as a producer of inflammatory cytokines and on their proinflammatory role. However, a recent study has demonstrated a new role for platelets in the liver: that of platelet-derived serotonin mediating liver regeneration.[26] Moreover, it has been reported that TPO-induced thrombocytosis attenuates progression of liver fibrosis and accelerates liver fibrolysis.[27,28] However, the mechanisms remain obscure, and the extrathrombocytotic effect of TPO could not be excluded from their study results. In the present study, we were able to clearly demonstrate that platelets serve as antifibrotic cells in the liver via the HGF/Met pathway and offer the novel finding that thrombocytopenia exacerbates liver fibrosis in vivo.

To examine the impact of thrombocytopenia in liver fibrosis, we generated a novel mouse model of severe thrombocytopenia. Previous research has shown that platelets are genetically programmed to die in an apoptotic manner and that their life span is regulated by a fine balance between antiapoptotic Bcl-xL and proapoptotic Bak; mice lacking a single allele of the *bcl-x* gene develop mild thrombocytopenia, which is attenuated with a *bak* knockout background.[5] However, traditional knockout of both alleles of the *bcl-x* gene leads to embryonic lethality.[6] To develop severe thrombocytopenic mice without phenotype expression in other organs caused by Bcl-xL deficiency, we generated thrombocyte-specific Bcl-xL knockout mice by crossing *floxed bcl-x* mice[6,7] and transgenic mice expressing the Cre-recombinase under regulation of the promoter of the Pf4 gene.[8] The expression of Pf4 promoter is reported to be specific to thrombocytes,[8] and its specificity was also confirmed in our generated mice. The mice displayed severer thrombocytopenia than the single allele knockout mice, at as early as 4 weeks of age, and it persisted for a longer time (Supplementary Figure 3).

Thrombocytopenic mice did not develop any liver pathology under physiologic conditions but developed exacerbated liver fibrosis upon BDL. Similar exacerbation of liver fibrosis was found in another liver fibrosis model induced by chronic injection of carbon tetrachloride (Supplementary Figure 4). Following BDL, thrombocytopenic mice showed lower ALT levels than the control mice. Because there was no significant difference in histologic necrosis and hepatocyte apoptosis between the 2 groups, the significance of this difference is obscure. Research has revealed proinflammatory roles of platelets in the liver under some experimental conditions.[23-25] Thus, thrombocytopenia might have led to modest reduction of liver injury in our experiment without any histologic differences. Even if that were the case, modest decline of liver injury could not explain the exacerbation of liver fibrosis in thrombocytopenic mice. It is well known that the liver has the unique capacity to regenerate in response to partial hepatectomy or some types of liver injury.[29] Recent research has shown that platelets mediate liver regeneration after partial hepatectomy.[26] In our experiment, modest compensatory regeneration did occur following BDL, but we could not find any difference in liver regeneration between the 2 groups. Following two thirds' partial hepatectomy, most hepatocytes in the remaining liver enter an active state of cell cycle progression,[29] whereas only a relatively small number of them may do so following liver injury. That may explain why liver regeneration did not differ in our models. Taken together, we considered that liver fibrosis is the primary and most prominent difference between the thrombocytopenic mice and the control littermates after BDL.

With regard to the underlying mechanisms of exacerbated liver fibrosis in thrombocytopenic mice upon BDL, we first took particular notice of the increase in collagen gene expression. In fact, liver fibrosis is known to be regulated by a fine balance between fibrogenesis and fibrolysis.[1,2] A variety of matrix metalloproteases (MMPs), such as MMP-2, MMP-9, and MMP-14, which may be involved in fibrolysis, were also up-regulated in the liver in thromobocytopenic mice compared with control mice (Supplementary Figure 5*A*). In addition, gene expression of platelet-derived growth factor, D polypeptide, transforming

Figure 5. The HGF/Met pathway is involved in platelet-mediated inhibition of collagen synthesis in HSCs in vitro. (*A*) *col1a1* And *col1a2* mRNA levels in HSCs stimulated with murine HGF for 6 hours by real-time reverse-transcription polymerase chain reaction, n = 3/group. $^*P < .05$ vs control. (*B*) Secretion of HGF from activated platelets. Platelets (1.0×10^7) were stimulated with or without thrombin (1 U/mL) for 15 minutes, and the levels of HGF in the culture supernatant were determined by ELISA, n = 3/group. $^*P < .05$ vs other 2 groups. (*C*) Production of HGF in platelet/HSC coculture. HSCs (1.0×10^5) were cocultured with 5.0×10^7 of platelets for 3 hours, and the levels of HGF in the culture medium were determined by ELISA, n = 3/group. $^*P < .05$ vs the other 2 groups. (*D*) Activation of Met and its downstream pathways in platelet/HSC coculture. HSCs (5.0×10^5) were cocultured with or without 5.0×10^7 platelets or with 20 ng/mL HGF as a positive control for 1 hour. Western blot analysis of phosphorylated Met protein at indicated position of tyrosine (*left panel*) and phosphorylated Erk1/2, Akt, and stat3 proteins (*right panel*). (*E*) Real-time reverse-transcription polymerase chain reaction (*upper panel*) and Western blot analysis (*lower panel*) of Met expression in HSCs transfected with *met* siRNA or control siRNA. (*F*) *col1a1* And *col1a2* mRNA levels in HSCs treated with *met* siRNA by real-time reverse-transcription polymerase chain reaction. HSCs were transfected with *met* siRNA or control siRNA for 3 days and then cultured for 6 hours with or without 20 ng/mL HGF (*left*) or with or without 1.0×10^7 platelets (*right*), n = 3/group.

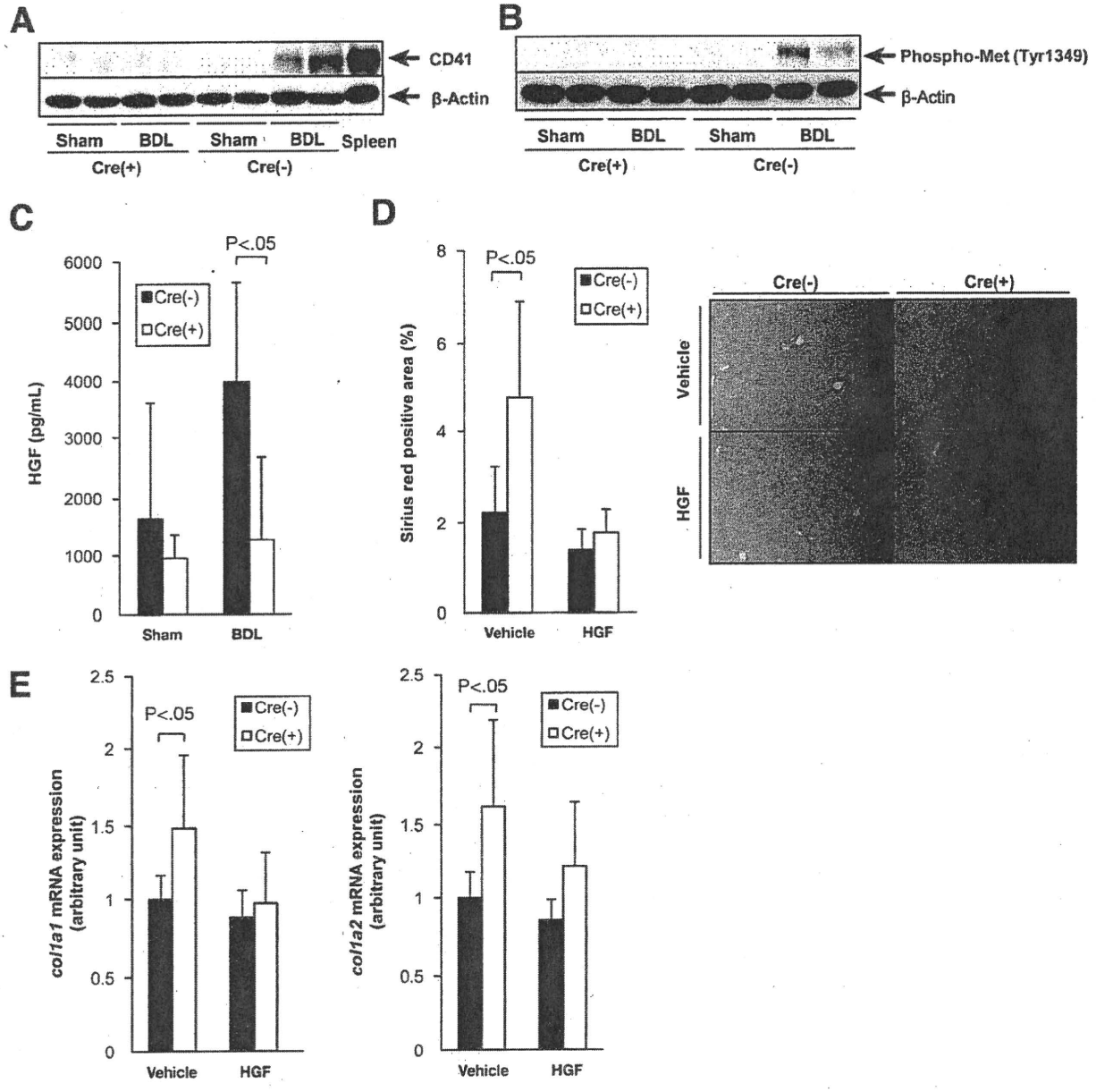

Figure 6. HGF administration prevents the exacerbation of liver fibrosis in the thrombocytopenic mice after BDL. (*A–C*) Platelet accumulation and Met activation in the liver following BDL. *bcl-x*$^{flo/xflox}$ *Pf4-Cre* mice and *bcl-x*$^{flox/flox}$ mice were sham operated or subjected to BDL and analyzed 10 days later (4–7 mice per group). Cre(+) stands for *bcl-x*$^{flox/flox}$ *Pf4-Cre* mice and Cre(−) for *bcl-x*$^{flox/flox}$ mice. Platelet accumulation in the liver was assessed by Western blotting of CD41 (*A*); lysate of spleen was used as a positive control. Phosphorylation of Met protein in the liver was determined by Western blot analysis (*B*). Plasma HGF levels were determined by ELISA (*C*). (*D* and *E*) Attenuation of liver fibrosis by HGF therapy in thrombocytopenic mice following BDL. *bcl-x*$^{flo/xflox}$ *Pf4-Cre* mice and *bcl-x*$^{flox/flox}$ mice were subjected to BDL, followed by intraperitoneal injection of recombinant human HGF or vehicle 2 times per day and analyzed 10 days later (5–7 mice per group). Liver fibrosis was evaluated by picrosirius red staining of liver sections (*D*). *co1a1* And *col1a2* mRNA in the liver were determined by real-time reverse-transcription polymerase chain reaction (*E*).

growth factor-β, and tumor necrosis factor-α, which are also known as cytokines involved in fibrosis, was not different between the 2 groups (Supplementary Figure 5*B*). These gene expression profiles suggest that increase of collagen gene expression may have a causative role in exacerbated liver fibrosis and that MMP up-regulation may be a compensatory phenomenon.

In general, according to the transdifferentiation of quiescent HSCs into activated HSCs, these myofibroblast-like cells express myogenic markers such as α-smooth muscle actin (SMA) and cause a parallel increase in collagen synthesis.[1,2] However, instead of increased collagen synthesis in thrombocytopenic mice, α-SMA positive cells were similarly induced in thrombocytopenic mice and control

mice upon BDL (Supplementary Figure 6). Thereafter, we expected that the levels of collagen gene expression per cell would increase in thrombocytopenic mice. Previous research has demonstrated that, even in activated HSCs, the level of type I collagen mRNA can be modulated by the change of collagen mRNA stabilization, which is regulated by interaction with a specific protein such as α complex protein.[30] Furthermore, it has recently been demonstrated that HGF suppresses *col1a2* promoter activation by inhibiting nuclear accumulation of Smad3 in activated HSCs.[31] We used activated HSCs for in vitro experiments and found that coculture with platelets did not affect mRNA expression of α-SMA (Supplementary Figure 7) but did suppress the *col1a1* and *col1a2* genes in activated HSCs. This suggests that platelets regulate type I collagen gene expression in each cell without affecting the activation status of HSCs, which agrees with our in vivo findings.

Platelet suppression of collagen gene expression was clearly associated with platelet activation as evidenced by the shape change and P-selectin translocation and shedding. Moreover, the supernatant of thrombin-activated platelets was capable of inhibiting collagen gene expression, although the supernatant of quiescent platelets could not. These results strongly suggest that platelet activation is indispensable for the inhibition of collagen synthesis in vitro. It should be noted that our results also suggest that, once activated, platelets are capable of releasing soluble factor(s) residing in platelet granules such as HGF and thereby suppress collagen synthesis, which is independent of how platelets are activated. Therefore, although platelets could be activated upon contact with HSCs in vitro, this contact may not be a requisite for platelet inhibition of HSCs in vivo. Indeed, platelets are well known to be activated by cell-to-cell contact with a variety of cells and soluble factors in injured organs.[10,14] We also observed that platelets could be activated upon contact with murine hepatocytes or macrophages in vitro, even though activated platelets did not affect type I collagen synthesis in these cells (data not shown).

We have demonstrated that platelet-derived HGF plays a critical role in platelet suppression of type I collagen gene expression in cultured HSCs. BDL-induced cholestasis led to intrahepatic platelet accumulation and Met phosphorylation in the liver of control mice, but both were attenuated in thrombocytopenic mice. Furthermore, plasma HGF levels in thrombocytopenic mice were lower than in control mice after BDL. Despite the lack of intrahepatic platelet accumulation, HGF administration could alleviate cholestasis-induced liver fibrosis in thrombocytopenic mice to the same level found in control mice. These findings implied that the lack of platelet-derived HGF signaling in the liver was involved in exacerbated liver fibrosis in thrombocytopenic mice. It is not clear, in the present study, whether cholestasis-induced Met phosphorylation in the liver originates from activated HSCs or just hepatocytes. Therefore, it is quite possible that HGF administration alleviated liver fibrosis by stimulating both hepatocytes and HSCs in thrombocytopenic mice. However, marked suppression of hepatic type I collagen gene expression by HGF therapy in thrombocytopenic mice suggests that attenuated Met phosphorylation and the subsequent increase of collagen synthesis in activated HSCs may be involved in exacerbated liver fibrosis in thrombocytopenic mice because collagen production is mainly mediated by activated HSCs in the injured liver.

HGF was first identified as a potent mitogen for primary hepatocytes after being purified from the plasma of a patient with fulminant hepatic failure[16,17] and also from rat platelets.[18] HGF is known to be a multifunctional growth factor that shows mitogenic, motogenic, morphogenic, and antiapoptotic activities in a variety of cells.[16,17] Increasing evidence indicates that HGF has an antifibrotic effect in several experimental models, especially when administered exogenously.[20,21] Although platelets are known to contain HGF in their granules,[18] the functional role of platelet-derived HGF has remained unknown. Because human platelets contain a smaller amount of HGF than rodent platelets,[18] it is obscure whether the same mechanisms observed in rodents are operative in humans. However, the present study, for the first time, sheds light on HGF derived from platelets serving as an endogenous negative regulator for HSC expression of collagen genes and liver fibrosis under pathologic conditions.

Thrombocytopenia is a common complication of advanced chronic liver disease and is generally considered to be a secondary phenomenon via associated portal hypertension or reduced production of TPO in the liver.[3,4] Our study indicates a causal link of thrombocytopenia with progression of liver fibrosis, suggesting a complicated interaction between liver fibrosis and thrombocytopenia. However, the mice we generated show extremely severe thrombocytopenia, which does not exactly mimic the thrombocytopenia usually seen in patients with cirrhosis. Moreover, the components of platelet granules may differ between the human and the mouse. Therefore, we cannot directly conclude from our findings that thrombocytopenia in patients with cirrhosis exacerbates liver fibrosis. However, in addition to the fact that liver fibrosis progresses in parallel with the decrease of platelet count, several studies on human patients have shown that splenectomy or partial splenic embolization can improve the liver function of cirrhotic patients in parallel with elevation of platelet count.[32,33] Therefore, further clinical study is important in order to elucidate whether an increase in platelet count is beneficial for preventing the progression of liver fibrosis in thrombocytopenic patients with advanced liver disease.

Supplementary Material

Note: To access the supplementary material accompanying this article, visit the online version of *Gastroenterology* at www.gastrojournal.org, and at doi: 10.1053/j.gastro.2010.02.054.

References

1. Bataller R, Brenner DA. Liver fibrosis. J Clin Invest 2005;115: 209–218.
2. Friedman SL. Mechanisms of hepatic fibrogenesis. Gastroenterology 2008;134:1655–1669.
3. Afdhal N, McHutchison J, Brown R, et al. Thrombocytopenia associated with chronic liver disease. J Hepatol 2008;48:1000–1007.
4. Aster RH. Pooling of platelets in the spleen: role in the pathogenesis of "hypersplenic" thrombocytopenia. J Clin Invest 1966;45: 645–657.
5. Mason KD, Carpinelli MR, Fletcher JI, et al. Programmed anuclear cell death delimits platelet life span. Cell 2007;128:1173–1186.
6. Takehara T, Tatsumi T, Suzuki T, et al. Hepatocyte-specific disruption of Bcl-xL leads to continuous hepatocyte apoptosis and liver fibrotic responses. Gastroenterology 2004;127:1189–1197.
7. Hikita H, Takehara T, Shimizu S, et al. Mcl-1 and Bcl-xL cooperatively maintain integrity of hepatocytes in developing and adult murine liver. Hepatology 2009;50:1217–1226.
8. Tiedt R, Schomber T, Hao-Shen H, et al. Pf4-Cre transgenic mice allow generating lineage-restricted gene knockouts for studying megakaryocyte and platelet function in vivo. Blood 2007;109: 1503–1506.
9. Tsukamoto H, Matsuoka M, French SW. Experimental models of hepatic fibrosis: a review. Semin Liver Dis 1990;10:56–65.
10. Zarbock A, Polanowska-Grabowska RK, Ley K. Platelet-neutrophil-interactions: linking hemostasis and inflammation. Blood Rev 2007;21:99–111.
11. Bennet JS. Structure and function of the platelet integrin $\alpha IIb\beta 3$. J Clin Invest 2005;115:3363–3369.
12. Gujral JS, Liu J, Farhood A, et al. Reduced oncotic necrosis in Fas receptor-deficient C57BL/6J-lpr mice after bile duct ligation. Hepatology 2004;40:998–1007.
13. Friedman SL, Roll FJ, Boyles J, et al. Maintenance of differentiated phenotype of cultured rat hepatic lipocytes by basement membrane matrix. J Biol Chem 1989;264:10756–10762.
14. Holmsen H. Physiological functions of platelets. Ann Med 1989; 21:23–30.
15. Dunlop LC, Skinner MP, Bendall LJ, et al. Characterization of GMP-140 (P-selectin) as a circulating plasma protein. J Exp Med 1992;175:1147–1150.
16. Gohda E, Tsubouchi H, Nakayama H, et al. Purification and partial characterization of hepatocyte growth factor from plasma of a patient with fulminant hepatic failure. J Clin Invest 1988;81: 414–419.
17. Miyazawa K, Tsubouchi H, Naka D, et al. Molecular cloning and sequence analysis of cDNA for human hepatocyte growth factor. Biochem Biophys Res Commun 1989;163:967–973.
18. Nakamura T, Nishizawa T, Hagiya M, et al. Molecular cloning and expression of human hepatocyte growth factor. Nature 1989; 342:440–443.
19. Tulasne D, Foveau B. The shadow of death on the MET tyrosine kinase receptor. Cell Death Differ 2008;15:427–434.
20. Ueki T, Kaneda Y, Tsutsui H, et al. Hepatocyte growth factor gene therapy of liver cirrhosis in rats. Nat Med 1999;5:226–230.
21. Li Z, Mizuno S, Nakamura T. Antinecrotic and antiapoptotic effects of hepatocyte growth factor on cholestatic hepatitis in a mouse model of bile-obstructive diseases. Am J Physiol Gastrointest Liver Physiol 2007;292:G639–G646.
22. Giebeler A, Boekschoten MV, Klein C, et al. c-Met confers protection against chronic liver tissue damage and fibrosis progression after bile duct ligation in mice. Gastroenterology 2009;137: 297–308.
23. Iannacone M, Sitia G, Isogawa M, et al. Platelets mediate cytotoxic T lymphocyte-induced liver damage. Nat Med 2005;11: 1167–1169.
24. Lang PA, Contaldo C, Georgiev P, et al. Aggravation of viral hepatitis by platelet-derived serotonin. Nat Med 2008;14:756–761.
25. Laschke MW, Dold S, Menger MD, et al. Platelet dependent accumulation of leukocytes in sinusoids mediates hepatocellular damage in bile duct ligation-induced cholestasis. Br J Pharmacol 2008;153:148–156.
26. Lesurtel M, Graf R, Aleil B, et al. Platelet-derived serotonin mediates liver regeneration. Science 2006;312:104–107.
27. Murata S, Hashimoto I, Nakano Y, et al. Single administration of thrombopoietin prevents progression of liver fibrosis and promotes liver regeneration after partial hepatectomy in cirrhotic rats. Ann Surg 2008;248:821–828.
28. Watanabe M, Murata S, Hashimoto I, et al. Platelets contribute to the reduction of liver fibrosis in mice. J Gastroenterol Hepatol 2009;24:78–89.
29. Fausto N, Campbell JS, Riehle KJ. Liver regeneration. Hepatology 2006;43:S45–S53.
30. Stefanovic B, Hellebrand C, Holcik M, et al. Posttranscriptional regulation of collagen $\alpha 1(I)$ mRNA in hepatic stellate cells. Mol Cell Biol 1999;17:5201–5209.
31. Inagaki Y, Higashi K, Kushida M, et al. Hepatocyte growth factor suppresses profibrogenic signal transduction via nuclear export of smad3 with galectin-7. Gastroenterology 2008;134:1180–1190.
32. Murata K, Ito K, Yoneda K, et al. Splenectomy improves liver function in patients with liver cirrhosis. Hepatogastroenterology 2008;55:1407–1411.
33. Lee CM, Leung EK, Wang HJ, et al. Evaluation of the effect of partial splenic embolization of platelet values for liver cirrhosis patients with thrombocytopenia. World J Gastroenterol 2007;13: 619–622.

Received September 4, 2009. Accepted February 24, 2010.

Reprint requests

Address requests for reprints to: Norio Hayashi, MD, PhD, Department of Gastroenterology and Hepatology, Osaka University Graduate School of Medicine, 2-2 Yamada-oka, Suita, Osaka 565-0871, Japan. e-mail: hayashin@gh.med.osaka-u.ac.jp; fax: (81) 6-6879-3629.

Acknowledgments

The authors thank Radek Skoda (University Hospital Basel) and Lothar Hennighausen (National Institute of Health) for providing the *Pf4-Cre* mice and the *floxed bcl-x* mice, respectively.

T. Kodama and T. Takehara contributed equally to this work and share first authorship.

Conflicts of Interest

The authors disclose no conflicts.

Funding

Supported in part by a Grant-in-Aid for Scientific Research from the Ministry of Education, Culture, Sports, Science, and Technology, Japan (to T. Takehara), and a Grant-in-Aid from the Ministry of Health, Labour, and Welfare of Japan.

Supplementary Materials and Methods

Hematologic Analyses

Blood was collected from the inferior vena cava of mice. Complete blood cell counts were determined using an Automated Cell Counter (Sysmex, Kobe, Japan).

Histologic Analyses

The liver sections were stained with H&E or picrosirius red. The percentage of oncotic necrosis or fibrotic area was calculated using image analysis software (winROOF visual system; Mitani Co, Tokyo, Japan). To assess intrahepatic neutrophil accumulation, liver sections were stained with chloroacetate esterase, which is a specific marker of neutrophils,[1] using a Naphthol-ASD Chloroacetate Esterase Kit (Sigma–Aldrich, St. Louis, MO). To detect apoptotic cells, the liver sections were also subjected to terminal deoxynucleotidyl transferase-mediated deoxyuridine triphosphate nick-end labeling staining as previously reported.[2] To assess regenerative status, nuclear 5-bromo-2-deoxyuridine incorporation was evaluated as previously described.[3]

Determination of Liver Hydroxyproline Content

Hydroxyproline content was determined essentially as described previously.[4] Results are expressed as micrograms of hydroxyproline per gram of wet liver.

Isolation and Culture of Mouse Hepatic Stellate Cell

Hepatic stellate cell (HSCs) were isolated from C57BL/6J mice by 2-step collagenase-pronase perfusion of mouse liver followed by density gradient centrifugation with 8.2% Nycodenz (Sigma-Aldrich) as previously described.[5] Isolated HSCs were maintained at 37°C under 5% CO_2 in Dulbecco's modified Eagle medium containing 10% fetal calf serum. Activated HSCs after a few passages were used for the experiments unless otherwise indicated.

Cell Isolation

Monocytes and T lymphocytes were isolated from spleens of *bcl-x$^{flox/flox}$ Pf4-Cre* mice and *bcl-x$^{flox/flox}$* mice by magnetic cell sorting using magnetic beads (MACS; Miltenyi Biotec, Gladbach, Germany) with CD11b and CD90.2 antibodies according to the manufacturer's protocol. Abdominal macrophages were collected from these mice 5 days after intraperitoneal injection of 50 μL/g body weight thioglycollate broth (Sigma–Aldrich) by peritoneal lavage. Hepatocytes and nonparenchymal cells were isolated from those mice by collagenase perfusion of mouse liver followed by centrifugation.

Platelet Isolation

Platelets were isolated as described previously.[6] Briefly, whole blood collected from the inferior vena cava of C57BL/6J mice was mixed with one fourth volume of citrate phosphate dextrose (Sigma–Aldrich). Platelet-rich plasma was obtained by centrifugation at 100*g* for 15 minutes at room temperature without braking. After incubation with 1 μmol/L prostaglandin E_1 (Sigma-Aldrich) and 1 U/mL apyrase (Sigma–Aldrich), the platelets were isolated by centrifugation at 200*g* at room temperature for 15 minutes.

Western Blot Analysis

Western blotting was performed as previously described.[2] A detailed description of the antibodies used is provided in Supplementary Table 1.

Real-Time Reverse-Transcription Polymerase Chain Reaction

Total RNA extracted from the liver tissue and HSCs were reverse transcribed and subjected to real-time reverse-transcription polymerase chain reaction as previously described.[2] mRNA expression of the specific genes was quantified using TaqMan Gene Expression Assays (Applied Biosystems Inc, Foster City, CA). Assay IDs of the specific genes are provided in Supplementary Table 2. Transcript levels are presented as fold induction.

Small Interfering RNA-Mediated Knockdown

Cultured HSCs were transfected with small interfering RNA against *met* (Stealth RNAi, Oligo ID:MSS206635) (Invitrogen, Carlsbad, CA) using lipofectamine RNAi-MAX (Invitrogen) according to the manufacturer's protocol. Stealth RNA: Negative Control Low GC Duplex (Invitrogen) was used as the control.

Flow Cytometry

Isolated platelets were surface-stained with a fluorescein isothiocyanate-conjugated rat anti-mouse CD62p (P-selectin) antibody (BD Biosciences, Franklin Lakes, NJ). Samples were analyzed with a Becton Dickinson FACSCalibur flow cytometer (BD Biosciences), and the data were processed with the CELLQuest software (BD Biosciences).

Enzyme-Linked Immunosorbent Assay

Mouse HGF and soluble CD62p (P-selectin) levels in plasma and culture supernatant were measured by using DuoSet enzyme-linked immunosorbent assay mouse hepatocyte growth factor (HGF) and CD62p (R&D Systems, Minneapolis, MN), respectively, according to the manufacturer's protocol.

HGF Treatment

Wild-type (*bcl-x$^{fl/fl}$*) and knockout (*bcl-x$^{fl/fl}$ Pf4-Cre*) mice were subjected to bile duct ligation, followed by intraperitoneal injection of recombinant human HGF (500 μg/kg) or vehicle every 12 hours for 10 days and then killed to sample the liver tissues.

References

1. Gujral JS, Liu J, Farhood A, et al. Reduced oncotic necrosis in Fas receptor-deficient C57BL/6J-lpr mice after bile duct ligation. Hepatology 2004;40:998–1007.
2. Hikita H, Takehara T, Shimizu S, et al. Mcl-1 and Bcl-xL cooperatively maintain integrity of hepatocytes in developing an adult murine liver. Hepatology 2009;50:1217–1226.
3. Lesurtel M, Graf R, Aleil B, et al. Platelet-derived serotonin mediates liver regeneration. Science 2006;312:104–107.
4. Takehara T, Tatsumi T, Suzuki T, et al. Hepatocyte-specific disruption of Bcl-xL leads to continuous hepatocyte apoptosis and liver fibrotic responses. Gastroenterology 2004;127:1189–1197.
5. Seki E, De Minicis S, Osterreicher CH, et al. TLR4 enhances TGF-β signaling and hepatic fibrosis. Nat Med 2007;13:1324–1332.
6. Iannacone M, Sitia G, Isogawa M, et al. Platelets mediate cytotoxic T lymphocyte-induced liver damage. Nat Med 2005;11:1167–1169.

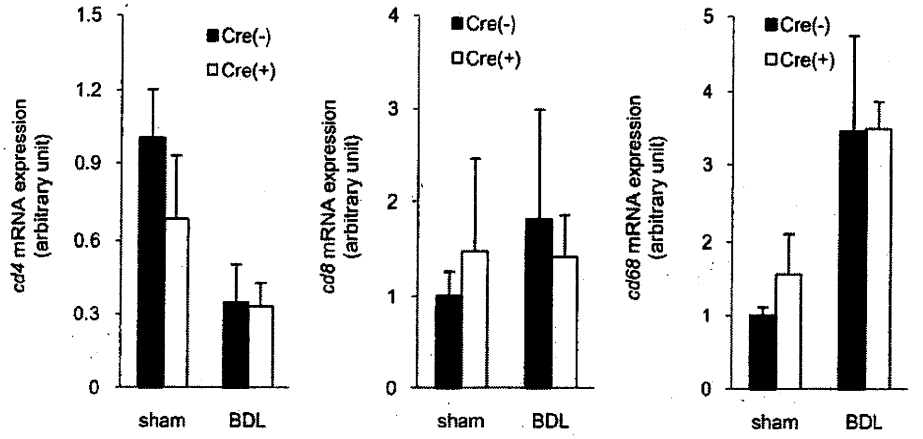

Supplementary Figure 1. Intrahepatic cell fractions upon bile duct ligation (BDL) treatment are not different between the thrombocytopenic mice and the control littermates. *bcl-x*$^{flox/flox}$ *Pf4-Cre* mice and *bcl-x*$^{flox/flox}$ mice were sham operated or subjected to BDL and analyzed 10 days later (4–6 mice per group). Cre(+) and Cre(−) stand for *bcl-x*$^{flox/flox}$ *Pf4-Cre* and *bcl-x*$^{flox/flox}$, respectively. *cd4*, *cd8*, And *cd68* messenger RNA levels in the liver were determined by real-time reverse-transcription polymerase chain reaction.

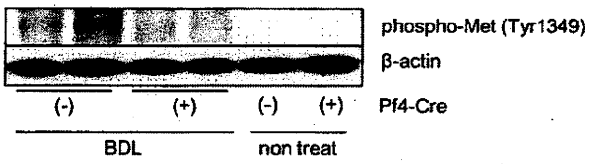

Supplementary Figure 2. Phosphorylation of Met protein in the liver is stronger in the control littermates than in the thrombocytopenic mice at 3 days after bile duct ligation (BDL) treatment. *bcl-x*$^{flox/flox}$ *Pf4-Cre* mice and *bcl-x*$^{flox/flox}$ mice were subjected to BDL and analyzed 3 days later. Cre(+) and Cre(−) stand for *bcl-x*$^{flox/flox}$ *Pf4-Cre* and *bcl-x*$^{flox/flox}$, respectively. Phosphorylation of Met protein in the liver was determined by Western blotting.

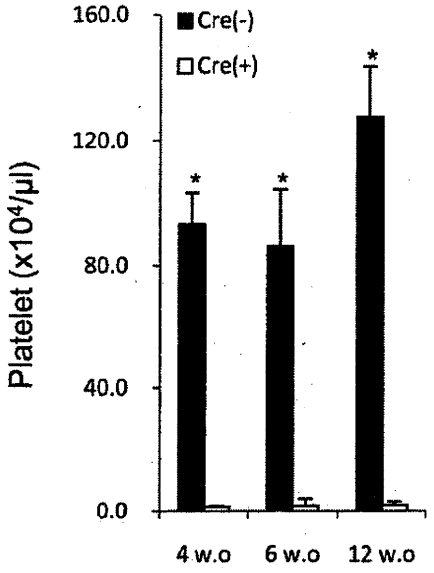

Supplementary Figure 3. *bcl-x*$^{flox/flox}$ *Pf4-Cre* mice exhibit severe thrombocytopenia at as early as 4 weeks of age, and it persists for a longer time. Circulating platelet counts of *bcl-x*$^{flox/flox}$ *Pf4-Cre* mice and *bcl-x*$^{flox/flox}$ mice at the age of 4, 6, and 12 weeks. Cre(+) and Cre(−) stand for *bcl-x*$^{flox/flox}$ *Pf4-Cre* and *bcl-x*$^{flox/flox}$, respectively. *$P < .05$ vs Cre(+). 5–8 Mice per group.

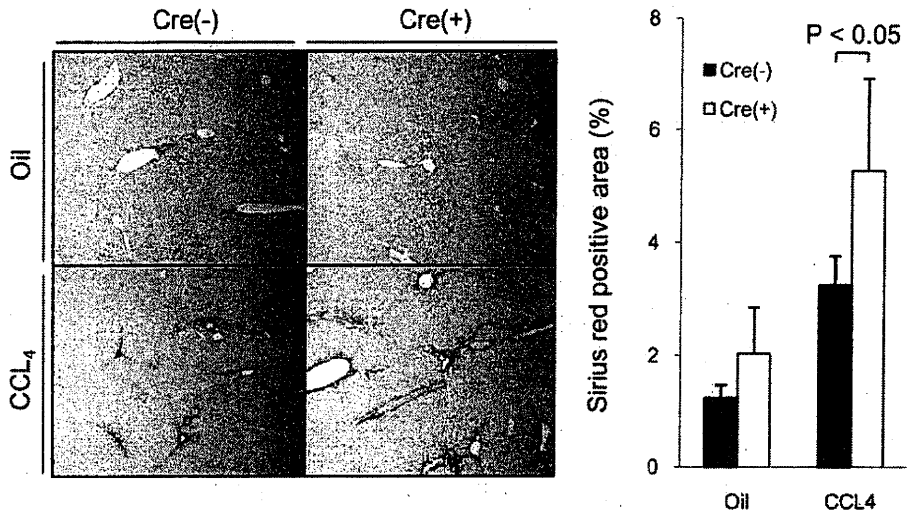

Supplementary Figure 4. Thrombocytopenia exacerbates liver fibrosis induced by chronic CCl_4 administration. *bcl-x*$^{flox/flox}$ *Pf4-Cre* mice and *bcl-x*$^{flox/flox}$ mice were administered intraperitoneal injection of CCl_4 (0.3 mL/kg) or oil 2 times per week and examined 6 weeks later (7 mice per group). Cre(+) and Cre(−) stand for *bcl-x*$^{flox/flox}$ *Pf4-Cre* and *bcl-x*$^{flox/flox}$, respectively. Liver fibrosis was evaluated by picrosirius red staining of liver sections.

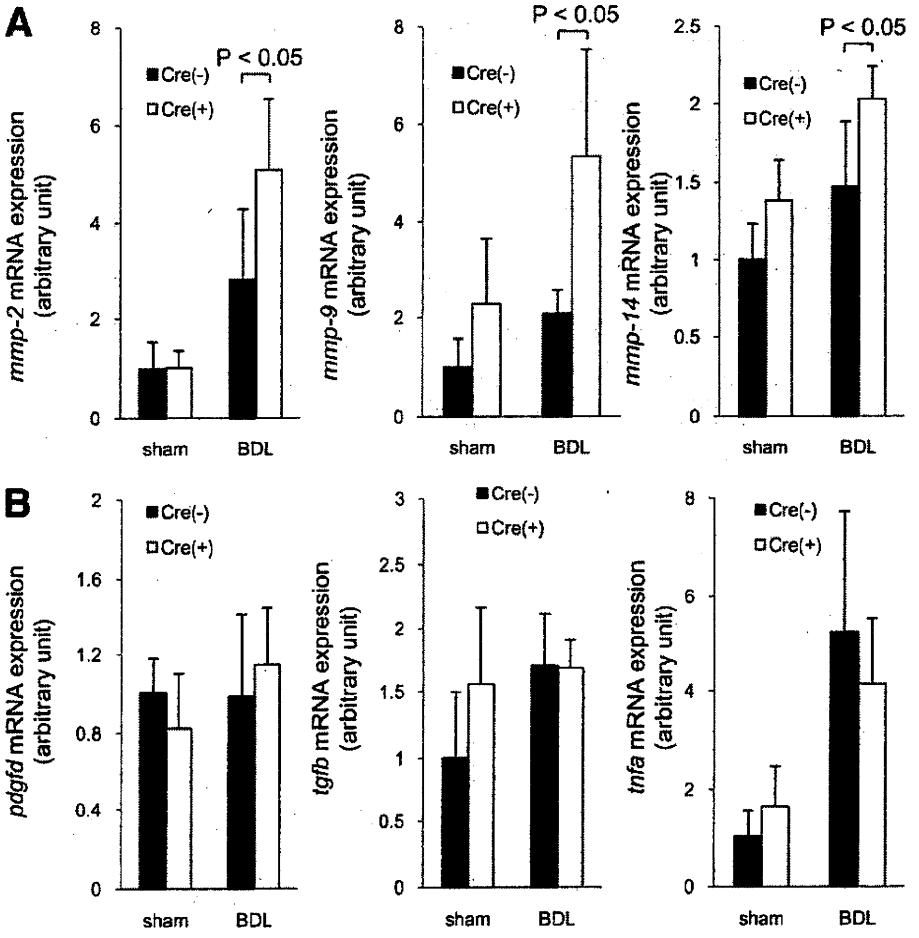

Supplementary Figure 5. (*A*) Gene expression of matrix metalloproteases is up-regulated in thrombocytopenic mice upon bile duct ligation (BDL) treatment. *bcl-x*$^{flox/flox}$ *Pf4-Cre* mice and *bcl-x*$^{flox/flox}$ mice were sham operated or subjected to BDL and analyzed 10 days later (4–6 mice per group). Cre(+) and Cre(−) stand for *bcl-x*$^{flox/flox}$ *Pf4-Cre* and *bcl-x*$^{flox/flox}$, respectively. *mmp-2*, *mmp-9*, And *mmp-14* messenger RNA levels in the liver were determined by real-time reverse-transcription polymerase chain reaction. (*B*) Gene expression of fibrosis-related cytokines in the liver is not different between the thrombocytopenic mice and their control littermates. *bcl-x*$^{flox/flox}$ *Pf4-Cre* mice and *bcl-x*$^{flox/flox}$ mice were sham operated or subjected to BDL and analyzed 10 days later (4–6 mice per group). Cre(+) and Cre(−) stand for *bcl-x*$^{flox/flox}$ *Pf4-Cre* and *bcl-x*$^{flox/flox}$, respectively. *pdgfd, tgfb, and tnfa* messenger RNA levels in the liver were determined by real-time reverse-transcription polymerase chain reaction.

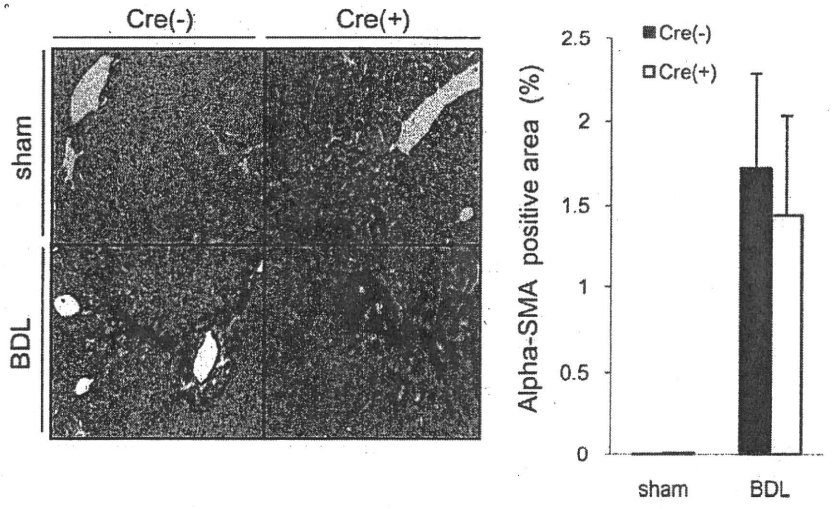

Supplementary Figure 6. HSCs are similarly activated in the thrombocytopenic mice and the control mice upon bile duct ligation (BDL). *bcl-x*$^{flox/flox}$ *Pf4-Cre* mice and *bcl-x*$^{flox/flox}$ mice were sham operated or subjected to BDL and analyzed 10 days later (4 or 5 mice per group). Cre(+) and Cre(−) stand for *bcl-x*$^{flox/flox}$ *Pf4-Cre* and *bcl-x*$^{flox/flox}$, respectively. To assess HSC activation, liver sections were stained with monoclonal anti-α-smooth muscle actin (α-*SMA*) (Dako, Glostrup, Denmark).

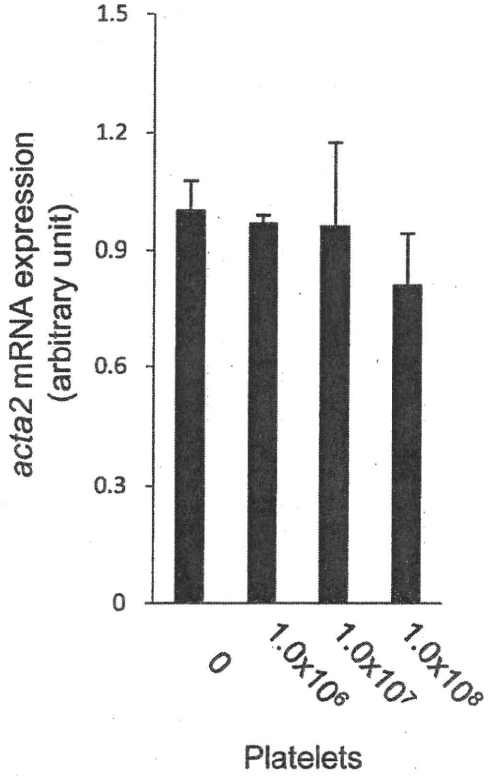

Supplementary Figure 7. Coculture with platelets does not affect messenger RNA expression of α-SMA in activated HSCs. HSCs (1.0×10^5) were cocultured with indicated dosages of platelets for 6 hours. *acta2* Messenger RNA levels in HSCs were determined by real-time reverse-transcription polymerase chain reaction. N = 3/group.

Supplementary Table 1. Antibodies Used for Western Blotting

Antibody	Manufacturer
Rabbit polyclonal antibody to Bcl-xL	Santa Cruz Biotechnology, Santa Cruz, CA
Rat monoclonal antibody to mouse integrin-α2B/CD41	R&D Systems, Minneapolis, MN
Mouse monoclonal antibody to Met	Cell Signaling Technology, Beverly, MA
Rabbit monoclonal antibody to phospho-Met (Tyr1234)	Cell Signaling Technology
Rabbit monoclonal antibody to phospho-Met (Tyr1349)	Cell Signaling Technology
Mouse monoclonal antibody to β-actin	Sigma-Aldrich, St Louis, MO
Rabbit polyclonal antibody to type I collagen	Rockland, Gilbertsville, PA
Rabbit polyclonal antibody to GAPDH	Trevigen, Gaithersburg, MD
Rabbit monoclonal antibody to stat3	Cell Signaling Technology
Rabbit monoclonal antibody to Erk1/2	Cell Signaling Technology
Rabbit monoclonal antibody to Akt	Cell Signaling Technology
Rabbit monoclonal antibody to phospho-stat3	Cell Signaling Technology
Rabbit monoclonal antibody to phospho-Ekr1/2	Cell Signaling Technology
Rabbit monoclonal antibody to phospho-Akt	Cell Signaling Technology

Supplementary Table 2. Clinicopathologic Features of HCC Patients

Target gene	Assay ID
col1a1	Mm00801666_g1
col1a2	Mm01165187_m1
met	Mm01156980_m1
mmp-2	Mm00439506_m1
mmp-9	Mm00600164_g1
mmp-14	Mm01318969_g1
acta2	Mm01546133_m1
actb	Mm02619580_g1
cd4	Mm01182108_m1
cd8	Mm00442754_m1
cd68	Mm03047343_m1
Tnfa	Mm01178820_m1
tgfb	Mm00546829_m1
pdgfd	Mm01135193_m1

Biochemical and Biophysical Research Communications 394 (2010) 87–93

Contents lists available at ScienceDirect

Biochemical and Biophysical Research Communications

journal homepage: www.elsevier.com/locate/ybbrc

Fatal exacerbation of type B chronic hepatitis triggered by changes in relaxed circular viral DNA synthesis and virion secretion

Kazuyoshi Ohkawa [a,b], Tetsuo Takehara [a], Hisashi Ishida [a], Takahiro Kodama [a], Satoshi Shimizu [a], Hayato Hikita [a], Masashi Yamamoto [a], Keisuke Kohga [a], Akira Sasakawa [a], Akio Uemura [a], Ryotaro Sakamori [a], Shinjiro Yamaguchi [a], Wei Li [a], Atsushi Hosui [a], Takuya Miyagi [a], Tomohide Tatsumi [a], Kazuhiro Katayama [b], Norio Hayashi [a,*]

[a] Department of Gastroenterology and Hepatology, Osaka University Graduate School of Medicine, 2-2, Yamadaoka, Suita 565-0871, Japan
[b] Department of Hepatobiliary and Pancreatic Oncology, Osaka Medical Center for Cancer and Cardiovascular Diseases, 1-3-3, Nakamichi, Higashinari-ku, Osaka 537-8511, Japan

ARTICLE INFO

Article history:
Received 11 February 2010
Available online 20 February 2010

Keywords:
Hepatitis B Virus
Fatal exacerbation of type B chronic hepatitis
Relaxed circular hepatitis B virus DNA synthesis
Virion secretion

ABSTRACT

Virological features of fulminant liver disease-causing hepatitis B virus (HBV) have not been fully elucidated. We studied longitudinally the viruses obtained before and after fulminant liver disease in a patient with chronic HBV infection showing fatal exacerbation. HBV strains were obtained before and after exacerbation (designated as FEP1 and FEP2). Their virological features were investigated by *in vitro* transfection. FEP1 and FEP2 possessed higher activity of overall HBV DNA synthesis than the wild-type. FEP1 lacked competence for relaxed circular (RC) HBV DNA synthesis and RC HBV DNA-containing virion secretion, but FEP2 maintained it. Chimeric analysis revealed that the preS/S gene, where FEP1 had a considerable number of mutations and deletions but FEP2 did not, was responsible for impaired RC HBV DNA synthesis and virion secretion. Furthermore, incompetence of FEP1 strain was transcomplemented by the preS/S protein of wild-type strain. In conclusion, the viral strain after exacerbation showed resurgent RC HBV DNA synthesis and virion secretion, which was caused by conversion of the preS/S gene from a hypermutated to hypomutated state. This may have been responsible for disease deterioration in the patient. This is a novel type of HBV genomic variation associated with the development of fulminant liver disease.

1. Introduction

Type B fulminant hepatitis develops in approximately 1% of patients with acute hepatitis B virus (HBV) infection and results in a high rate of mortality [1]. Serious disease exacerbation like fulminant hepatitis can also occur during chronic HBV infection. The virological characteristics of fulminant hepatitis-causing HBV strains have been widely studied. An A1896 mutation in the precore gene, and T1762/A1764 and V1753/V1754 mutations (V = not T) in the core promoter have been shown to be detected more frequently in fulminant hepatitis-related strains than in non-fulminant hepatitis-related ones [2–4], although these viral mutations do not completely account for the pathogenesis of fulminant hepatitis. A few investigators have conducted detailed studies on the strain-specific virological feature of an individual fulminant hepatitis-causing HBV strain in comparison with the representative wild-type HBV strain [5–8]. Baumert et al. [5,6] reported that a fulminant hepatitis-causing HBV strain with rare types of mutations in the core promoter showed a robust increase of viral encapsidation and strong induction of cellular apoptosis. Pult et al. [7] also revealed that the strain isolated from a patient with heart transplantation-associated fulminant hepatitis had the 11-bp insertion in the core promoter and revealed the elevated viral transcription via generation of a novel binding site of hepatocyte nuclear factor 1. In addition, Kalinina et al. [8] reported that the strain derived from a fulminant hepatitis patient after liver transplantation was secretion-defective due to several mutations in the surface (S) gene. According to these observations, in fulminant hepatitis-causing HBV strains, both frequent mutations and strain-specific viral genomic variations may contribute to the development of the disease. However, there have been no longitudinal virological studies of HBV strains obtained before and after the onset of fulminant liver disease in chronic HBV carriers showing serious disease exacerbation such as fulminant hepatitis. Such investigations may lead to better understanding of the role of viral genomic changes on the pathogenesis of HBV-related fulminant liver disease.

HBV is a double-stranded circular DNA virus approximately 3.2 kb long and has four open reading frames, preS/S, precore/core,

* Corresponding author.
E-mail address: hayashin@gh.med.osaka-u.ac.jp (N. Hayashi).

0006-291X/$ - see front matter © 2010 Elsevier Inc. All rights reserved.
doi:10.1016/j.bbrc.2010.02.114

polymerase and X genes. HBV replicates its genome via reverse transcription of pregenome RNA. Reverse transcription conducted by viral polymerase takes place after encapsidation of pregenome RNA, resulting in minus-strand DNA synthesis. The RNA template is simultaneously degraded by RNaseH activity, and single-stranded (SS) HBV DNA is constructed. Subsequently, viral polymerase mediates production of plus-strand DNA from minus-strand DNA. In this process, appropriate template switches for primer translocation and circularization lead to the formation of relaxed circular (RC) HBV DNA, whereas the extension *in situ* without template switches results in the formation of duplex linear (DL) HBV DNA [9–11]. The virion containing RC viral DNA has been shown to be more infectious than those containing DL viral DNA in duck hepatitis B virus (DHBV) [12].

In this study, we examined an elderly patient with chronic HBV infection showing fatal exacerbation accompanied by an increase in the viral replicative level. The viruses obtained before and after exacerbation were longitudinally studied. The virus before exacerbation lacked competence for RC HBV DNA synthesis and virion secretion, but the virus after exacerbation had recovered it. Resurgent RC HBV DNA synthesis and virion secretion as the prime causes of disease deterioration originated in conversion of the preS/S gene from a hypermutated to a hypomutated state. This is a novel type of the HBV genomic variation associated with the development of HBV-related fulminant liver disease.

2. Materials and methods

2.1. Case presentation

The patient described in this study was a 83-year-old Japanese male with type B chronic hepatitis. At the initial phase, he was free of symptoms. His alanine aminotransferase (ALT) fluctuated over a range of 50–160 IU/l. Hepatitis B surface antigen (HBsAg) was weakly positive (2^5 according to reversed passive hemagglutination assay), and HBV DNA was below the detection limit based on the slot–blot hybridization assay on day 29. However, after 1 year, he suddenly became fatigued and anorexic. ALT rose to 729 IU/l accompanied by an increase of HBsAg titer ($>2^{12}$) and the detectable level of HBV DNA on day 374. He was hospitalized due to diagnosis of acute exacerbation of chronic HBV infection. After hospitalization, ALT declined to 150–250 IU/l, but HBV DNA continued to be detectable. The total bilirubin reached up to 5.0 mg/dl on day 418 and increased thereafter. On day 508, he died of hepatic failure despite intensive treatment. Liver histology at autopsy showed features of massive liver necrosis superimposed on chronic non-cirrhotic liver disease. During follow-up, he tested negative for both hepatitis B e antigen (HBeAg) and antibody to HBeAg by radioimmunoassay. Antibody to HBsAg was also negative according to passive hemagglutination assay. The clinical course of the patient is summarized in Fig. 1. Informed consent was obtained from his family members. Serum samples collected on day 29 (1 year before exacerbation, designated as P1) and day 407 (after exacerbation, designated as P2) were stored at −80 °C and used for this study. HBV DNA levels as measured by the PCR-based assay (Amplicor HB Monitor, Roche Diagnostics) using stored sera at P1 and P2 were $10^{5.4}$ and $10^{8.6}$ copies/ml.

2.2. PCR, sequencing and subcloning

To obtain the full-length HBV DNA strains before and after exacerbation, PCR reaction was carried out using stored sera at P1 and P2. After DNA extraction, the DNA was amplified for 35 cycles using Taq/Pwo DNA polymerase (Roche Diagnostics) according to the method described by Günther et al. [13]. The primers were BF1 (5′-CCGGAAAGCTTGAGCTCTTCTTTTTCACCTCTGCCTAATCA-3′, nt 1821–1841) and BR1 (5′-CCGGAAAGCTTGAGCTCTTCAAAAAG TTGCATGGTGCTGG-3′, nt 1825–1806), both of which had a SapI recognition site at the 5′ end. After brief incubation with Taq polymerase to create A overhang, the PCR product was cloned into the plasmid pCR-TOPO4 (Invitrogen). To avoid misreading in the PCR reaction, nucleotide sequences of six independent full-length HBV DNA clones were determined. Nucleotides that were detected in only one clone at the corresponding nucleotide position were excluded. If necessary, the interchange in the portion of HBV DNA using plural number of clones, or site-directed mutagenesis,

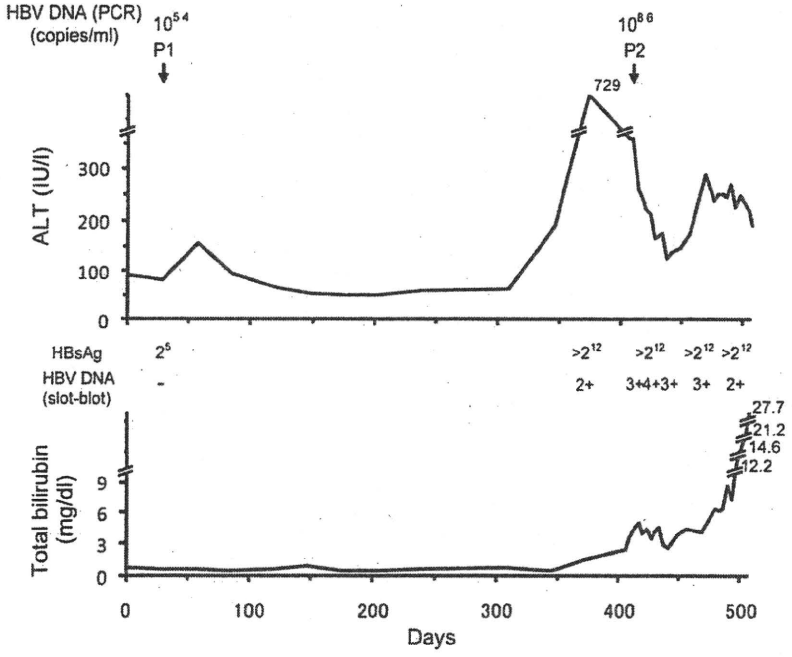

Fig. 1. Clinical course of a patient with type B chronic hepatitis showing fatal exacerbation.

was conducted. Finally, the HBV strains, FEP1 and FEP2 (GenBank Accession Nos. AB485809 and AB485810), were obtained as predominant viruses at P1 and P2. These two HBV strains were subjected to phylogenetic tree analysis along with representative HBV strains of various genotypes.

2.3. Plasmid constructs

Plasmid pHBC had 1.2 times the genomic length of HBV DNA and expressed the wild-type genotype C HBV strain adr4 (GenBank Accession No. X01587) [14]. As for the HBV strains FEP1 and FEP2, the full-length HBV DNA fragment was removed from the pCR-TOPO4 by SapI digestion, followed by synthesis of circular double-stranded HBV DNA by T4 ligase treatment. Based on this, the HBV-expressing plasmids pFEP1 and pFEP2, which carried the 1.2-fold HBV genome, were constructed. pFEch1 and pFEch2, made by swapping the BstEII/BstBI fragment between pFEP1 and pFEP2, expressed the chimeric HBV strains FEch1 and FEch2. For trans-complementation analysis, another plasmid pHBV1.5, which expressed wild-type genotype A HBV strain adw2 (GenBank Accession No. X02763) [15], was used. pHBV1.5Δpol and pHBV1.5ΔS lacked production of the polymerase protein and all surface proteins, respectively, due to insertion of the in-frame stop codon. pCMV-SEAP expressed a secreted alkaline phosphatase.

2.4. Examination for mixed viral population

To examine the mixed viral population in the preS/S gene, PCR-subcloning analysis was performed. The DNA fragment encompassing the whole preS2/S gene was amplified by PCR using the primers BF5 (5′-AAGAGACAGTCATCCTCAGG-3′ nt 3183–3202) and BR7 (5′-GGGTTCAAATGTATACCCAA-3′, nt 839–820). The PCR

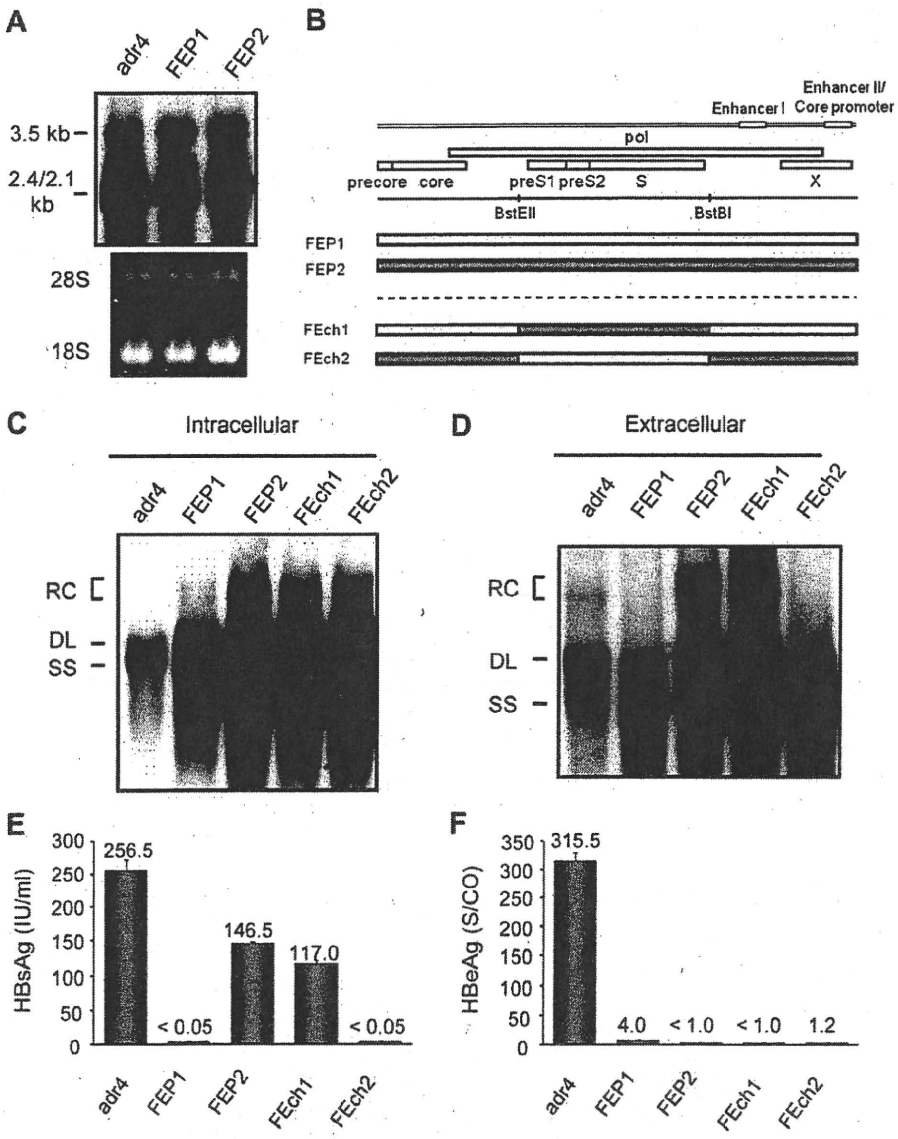

Fig. 2. Viral transcription, replication, virion secretion and antigen production of FEP1 and FEP2, and their chimeric constructs in transfected cells. (A) HBV transcripts in transfected cells examined by Northern blot analysis. The lower panel indicates ethidium bromide staining as a loading control. (B) A scheme of chimeric HBV strains, FEch1 and FEch2. (C) Intracellular progeny HBV DNA in transfected cells examined by Southern blot analysis. (D) Extracellular progeny HBV DNA in transfected cells examined by Southern blot analysis. (E) Secreted HBsAg in the culture supernatant of transfected cells. Data were expressed as IU/ml. (F) Secreted HBeAg in the culture supernatant of transfected cells. Data were expressed as the ratio of optical density of the sample to the cut-off value (S/CO). SS, single-stranded HBV DNA; DL, duplex linear HBV DNA; RC, relaxed circular HBV DNA.

product was cloned into the plasmid pCR-TOPO4, and inserted HBV DNA sequences of independent clones were determined. As another examination of the mixed viral population, PCR was done to obtain the short HBV DNA fragment including the preS2 deletion site using the primers BF-11 (5′-AAGAGACAGTCATCCTCAGG-3′, nt 3183–3202) and BR-11 (5′-AACTGGAGCCACCAGCAGGA-3′, nt 74–55). Next, the product was electrophoresed on polyacrylamide gel. In this assay, the various ratios of the mixture of plasmids pFEP1 and pFEP2 were used as templates of the PCR reaction. Consequently, a minor population of the virus could be detected if it was present at approximately one-tenth of the total population.

2.5. Transfection study

Huh7 cells (7×10^5 cells) were seeded on a 60-mm-diameter culture dish and transfected with 2 μg of various HBV-expressing plasmids and 0.1 μg of pCMV-SEAP using the FuGENE6 reagent (Roche Diagnostics). In transcomplementation analysis, 1 μg of pFEP1 was cotransfected with 1 μg of pHBV1.5Δpol, pHBV1.5ΔS or pBluescriptIISK$^+$ (mock). The cellular nucleic acid and culture supernatant were collected on day 5 after transfection. The alkaline phosphatase activity in the culture supernatant was measured to evaluate transfection efficiency.

For Northern blot analysis to detect HBV transcripts, the total RNA was extracted using an TRIzol reagent (Invitrogen), followed by RNase-free DNaseI treatment, phenol/chloroform extraction and ethanol precipitation. The sample was then electrophoresed in a formaldehyde–agarose denaturing gel, transferred onto a nylon membrane, hybridized with alkaline phosphatase-labeled HBV DNA probe and detected with the chemiluminescent substrate CDP-star (GE Healthcare Life Sciences). Southern blot analyses to detect intracellular and extracellular progeny HBV DNAs were carried out as described elsewhere [16]. Secreted HBsAg and HBeAg in the culture supernatant were measured by chemiluminescent immunoassay. All transfection experiments were done at least three times, and the representative results are shown.

3. Results

3.1. Differences in viral sequences between FEP1 and FEP2 strains were most prominent in the preS/S gene

The HBV strains FEP1 and FEP2, obtained before and after fatal exacerbation of the patient with chronic HBV infection, were classified as genotype C2, the most prevalent genotype in Japan, according to the phylogenetic tree analysis (data not shown). FEP1 and FEP2 had sequence divergences of 3.1% and 2.8% from the representative wild-type genotype C2 HBV strain adr4 [14] and differed by 0.8% from each other. Amino acid substitutions in the preS/S, precore/core, X and polymerase gene in adr4, FEP1 and FEP2 strains are shown in the Supplementary Tables 1 and 2. FEP1 had 20 amino acid substitutions in the preS/S gene, 6 in the precore/core gene, 5 in the X gene and 34 in the polymerase gene, whereas FEP2 had 10 in the preS/S gene, 7 in the precore/core gene, 5 in the X gene and 30 in the polymerase gene compared with adr4. As for comparison between FEP1 and FEP2, substitutions were noted at 15 amino acid residues in the preS/S gene, one in the precore/core gene, none in the X gene and 14 in the polymerase gene. In addition, FEP1, but not FEP2, had a 12-bp deletion in the preS2 gene, a 9-bp deletion in the S gene, and the in-frame stop codon in the distal S gene, which caused truncation of preS/S and polymerase proteins. As for other peculiarities of the FEP1 and FEP2 strains, both had the A1896, T1762/A1764 and C1753 mutations, which have been shown to be frequently detected in fulminant hepatitis [2–4], and disruption of the start codon of the preS2 gene, which has been reported to be commonly found in chronic HBV infection [17]. Thus, FEP1 and FEP2 strains differed considerably in nucleotide sequences from the wild-type adr4 strain. Further-

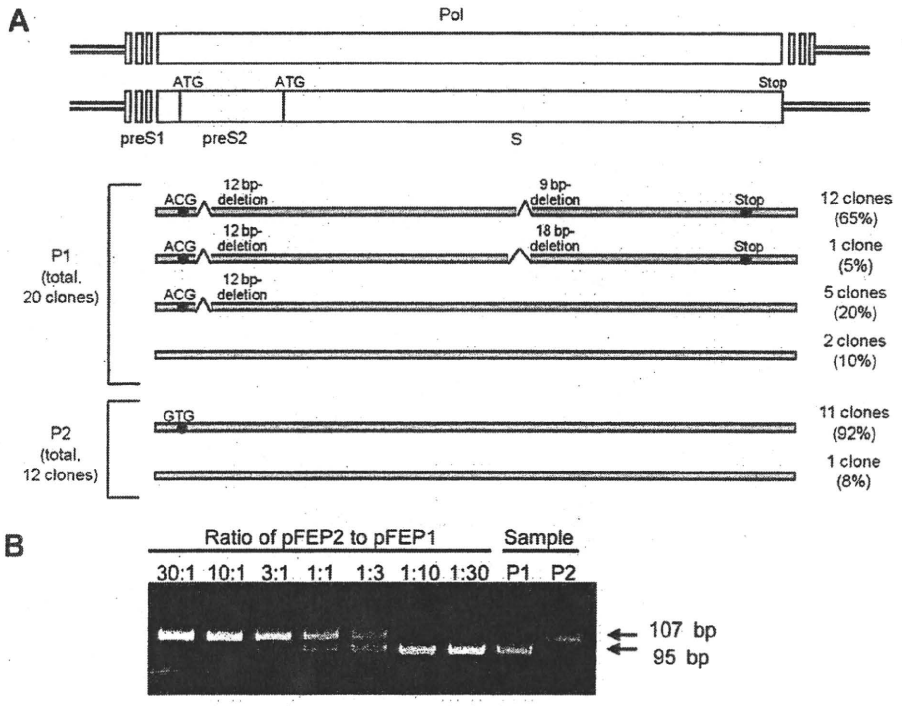

Fig. 3. Mixed viral population in the preS/S gene in a patient with type B chronic hepatitis showing fatal exacerbation. (A) A scheme of the result of PCR-subcloning analysis. The HBV fragment encompassing the whole preS2/S gene was amplified by PCR and subcloned. Next, the independent clones were used for sequencing analysis. A total of 20 and 12 independent clones derived from serum samples P1 and P2 were examined. (B) A representative result of PCR amplification of short HBV DNA fragment including the preS2 deletion site. The product derived from HBV DNA without the deletion was 109 bp long, whereas that derived from HBV DNA with the deletion was 95 bp long.

more, the differences between FEP1 and FEP2 in the sequences were the most prominent in the preS/S gene.

3.2. FEP1 lacked competence for RC HBV DNA synthesis and RC HBV DNA-containing virion secretion but FEP2 possessed it

Next, we investigated viral transcription, DNA synthesis, virion secretion and antigen production in the wild-type adr4 strain, and the patient-derived FEP1 and FEP2 strains using *in vitro* transfection analysis. The levels of HBV transcripts did not differ among the three strains (Fig. 2A). When the levels of intracellular and extracellular progeny HBV DNAs were compared (Fig. 2C and D), both FEP1 and FEP2 revealed more synthetic activity of HBV DNA than adr4 in the intracellular HBV DNA assay, but the differences in the levels of extracellular HBV DNA among adr4, FEP1 and FEP2 were modest. According to these findings, FEP1 and FEP2 strains may possess increased activity of viral encapsidation and/or minus-strand DNA synthesis compared with adr4, whereas wild-type adr4 strain may be superior to FEP1 and FEP2 in the efficient virion secretion. When the differences between FEP1 and FEP2 were examined with respect to the intracellular and extracellular HBV DNA assays, RC HBV DNA synthesis and RC HBV DNA-containing virion secretion were seriously impaired in FEP1, compared with FEP2 (Fig. 2C and D). Regarding the levels of secreted HBsAg and HBeAg, HBsAg was not detected in FEP1 but detectable in adr4 and FEP2 (Fig. 2E). Both FEP1 and FEP2 could not synthesize HBeAg (Fig. 2F), because they harbored the precore-defective A1896 mutation.

3.3. Inability of RC HBV DNA synthesis and of RC HBV DNA-containing virion secretion in FEP1 were responsible for the preS/S gene

The most remarkable difference in the viral genome between FEP1 and FEP2 was observed in the preS/S gene. Therefore, chimeric HBV strains, FEch1 and FEch2, constructed by swapping the entire preS/S region between FEP1 and FEP2 (Fig. 2B), were examined. As shown in Fig. 2C and D, RC HBV DNA synthesis and RC HBV DNA-containing virion secretion were seen in FEch1 but had been prevented in FEch2. Also, HBsAg was detected in FEch1 but not in FEch2 (Fig. 2E). Both FEch1 and FEch2 did not produce HBeAg (Fig. 2F). Thus, incompetence of RC HBV DNA synthesis and of virion secretion in FEP1 were responsible for the preS/S gene.

3.4. Wild-type-like HBV strain coexisted with FEP1 strain

We further examined the detailed viral population at P1 and P2. PCR-subcloning assay was done for the preS2/S gene, which showed the regions with the most differences in sequences between FEP1 and FEP2 (Fig. 3A). Thirteen of 20 clones derived from P1 had the two short deletions in the preS2 and S genes, the in-frame stop codon in the distal S gene and disruption of the preS2 start codon, as was the case for FEP1 strain. Five clones possessed only the deletion in the preS2 gene and disruption of the preS2 start codon. The remaining two clones had none of these mutations and deletions and were similar to the wild-type strain. As for clones derived from P2, 11 of the 12 clones showed disruption of the preS2 start codon, whereas the remaining one clone did not. In PCR analysis for the short region containing the preS2 deletion site (Fig. 3B), the virus with preS2 deletion was predominant, but approximately one-tenth of the virus without deletion was also detected at P1. Only the virus without the deletion was seen at P2. According to these observations, the wild-type-like HBV strain with minimal viral genomic variations in the preS/S gene coexisted as a minor population at P1.

3.5. RC HBV DNA synthesis and virion secretion were transcomplemented by the preS/S protein

Finally, we investigated whether the wild-type-like virus coexisting as a minor population can complement the inability of RC HBV DNA synthesis and virion secretion in FEP1 strain *in trans*. As shown in Fig. 4A, transfection with pHBV1.5 yielded synthesis of RC, DL and SS HBV DNAs, whereas transfection with pHBV1.5ΔS resulted in less amounts of RC HBV DNA than that with pHBV1.5. Transfection with pHBV1.5Δpol showed complete absence of HBV DNA synthesis. As for transcomplementation analysis (Fig. 4B and C), cotransfection of pHBV1.5Δpol with pFEP1 did not augment RC HBV DNA synthesis in the intracellular HBV DNA assay, but led to enhanced secretion of RC HBV DNA-containing virion in the extracellular HBV DNA assay. By contrast, cotransfec-

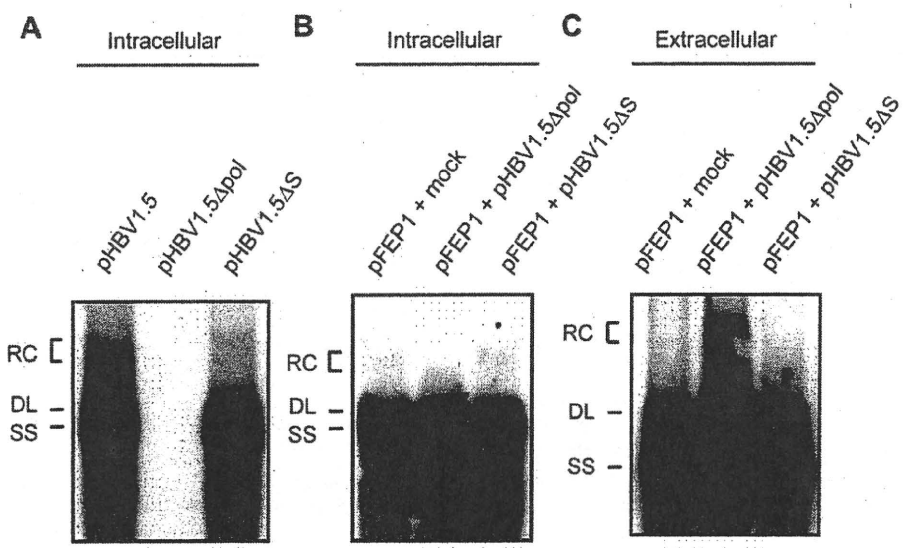

Fig. 4. Transcomplementation of insufficient viral secretion in FEP1 strain by HBV-expressing constructs, pHBV1.5Δpol and pHBV1.5ΔS. (A) Intracellular progeny HBV DNA in cells transfected with pHBV1.5, pHBV1.5Δpol and pHBV1.5ΔS by Southern blot analysis. (B) Intracellular progeny HBV DNA in cells cotransfected of pFEP1 with mock, pHBV1.5Δpol and pHBV1.5ΔS by Southern blot analysis. (C) Extracellular progeny HBV DNA in cells cotransfected of pFEP1 with mock, pHBV1.5Δpol and pHBV1.5ΔS by Southern blot analysis. SS, single-stranded HBV DNA; DL, duplex linear HBV DNA; RC, relaxed circular HBV DNA.

tion of pHBV1.5ΔS with pFEP1 could not compensate for the inability of RC HBV DNA synthesis and virion secretion. These results suggest that insufficiency of RC HBV DNA synthesis and virion secretion in FEP1 may be transcomplemented not by the polymerase protein but by the preS/S protein of the wild-type-like HBV strain.

4. Discussion

The present study describes a patient with type B chronic hepatitis who showed fatal exacerbation accompanied by more than 10^3-fold increment of viral replicative activity. The predominant HBV strains FEP1 and FEP2, obtained before and after exacerbation, were investigated to clarify what viral genomic alterations triggered disease deterioration. FEP1 and FEP2 possessed considerably different nucleotide sequences including A1896, T1762/A1764 and C1753 mutations, that have been reported to be frequently detected in the fulminant hepatitis-related HBV strain, compared with the wild-type strain [2–4]. Not only FEP2 and but also FEP1 revealed more overall synthetic activity of HBV DNA than the wild-type strain. Thus, both FEP1 and FEP2 were potent highly-replicative strains. As for the most significant difference between FEP1 and FEP2, FEP1 lacked competence for RC HBV DNA synthesis and RC HBV DNA-containing virion secretion, whereas FEP2 maintained it. Because of the difference in the virological feature between them, FEP1 was not very pathogenic, but FEP2 became a highly virulent strain. These results indicate that resurgent RC HBV DNA synthesis and virion secretion may lead to the onset of fulminant liver disease in this patient.

Chimeric analysis revealed that the preS/S gene, where FEP1 had a considerable number of mutations and deletions but FEP2 did not, accounted for the difference in the ability of RC HBV DNA synthesis and virion secretion between FEP1 and FEP2. In addition, insufficient RC HBV DNA synthesis and virion secretion in FEP1 were transcomplemented not by the polymerase protein but by the preS/S protein of the wild-type virus. Although mutations and deletions in the preS/S gene observed in FEP1 certainly affect the properties of both preS/S and polymerase proteins, disability of the preS/S protein rather than the polymerase protein may be responsible for the inability of RC HBV DNA synthesis and virion secretion in FEP1. By contrast, FEP2 may produce the competent preS/S protein to accomplish RC HBV DNA synthesis and virion secretion because of fewer mutations in the preS/S gene. Taken together, conversion from a hypermutated to a hypomutated state in the preS/S gene may have been the strain-specific viral genomic change serving as the primitive cause of lethal disease deterioration in our patient.

Examination for viral population showed that the wild-type-like strain carrying no mutations in the preS/S gene coexisted as a minor population with the predominant strain epitomized by FEP1 before exacerbation. Transcomplementation analysis also revealed that the wild-type-like HBV strain may function as a helper virus that compensates for impaired synthesis of RC HBV DNA and virion secretion in FEP1 strain. This may be a reason why the patient already had a certain degree of viral replication and chronic liver inflammation before exacerbation.

A few investigators reported secretion-defective HBV strains with the mutations in the S gene derived from patients with fulminant hepatitis and those with chronic HBV infection [8,18]. Regarding the former strain, the secretion-defective strain was isolated after the onset of fulminant hepatitis, suggesting the pathogenic importance of the deficiency in the viral antigen secretion itself [8]. This does not agree with our findings because the virus lacking the ability of RC HBV DNA-containing virion secretion was not very pathogenic, but the virus having it triggered fulminant liver disease in our study. Further work should be done to clarify the involvement of the secretion-defective HBV in various clinical manifestations.

In the process of plus-strand DNA synthesis, the presence or absence of template switches for primer translocation and circularization determines the preference for RC HBV DNA synthesis. Appropriate template switches and subsequent RC HBV DNA synthesis require donor and acceptor sites for template switches and several other *cis*-acting sequences [10,11]. FEP1 is, to our knowledge, the first naturally-occurring HBV strain displaying incompetence of RC HBV DNA synthesis and virion secretion. Such incompetence in FEP1 was compensated not by the polymerase protein but by the preS/S protein of the wild-type HBV. This lets us hypothesize that the preS/S protein may play a pivotal role in the secretion of RC HBV DNA-containing virus and possibly, the synthesis of RC HBV DNA. The preS/S protein, as well as the polymerase protein and *cis*-acting sequences within the viral genome, may be an important component for efficient RC HBV DNA formation. The hypothesis is also supported by our other finding that the synthetic activity of RC HBV DNA was lower in cells transfected with pHBV1.5ΔS than in those transfected with pHBV1.5.

In summary, we identified a novel type of the viral genomic variation associated with the development of fulminant liver disease in the longitudinal virological study of a type B chronic hepatitis patient showing fatal exacerbation. The virus before exacerbation revealed insufficiency of RC HBV DNA synthesis and virion secretion, but the virus after exacerbation had the ability for both. The change in the virological character was based on conversion from a hypermutated to a hypomutated status in the preS/S gene, which may be the main cause for disease deterioration in the patient. Our findings offer a new insight into the pathogenesis of HBV-related fulminant liver disease.

Appendix A. Supplementary data

Supplementary data associated with this article can be found, in the online version, at doi:10.1016/j.bbrc.2010.02.114.

References

[1] W.M. Lee, Acute liver failure, N. Engl. J. Med. 329 (1993) 1862–1872.
[2] M. Omata, T. Ehata, O. Yokosuka, K. Hosoda, M. Ohto, Mutations in the precore region of hepatitis B virus DNA in patients with fulminant and severe hepatitis, N. Engl. J. Med. 324 (1991) 1699–1704.
[3] S. Satō, K. Suzuki, Y. Akahane, K. Akamatsu, K. Akiyama, K. Yunomura, F. Tsuda, T. Tanaka, H. Okamoto, Y. Miyakawa, M. Mayumi, Hepatitis B virus strains with mutations in the core promoter in patients with fulminant hepatitis, Ann. Intern. Med. 122 (1995) 241–248.
[4] T. Imamura, O. Yokosuka, T. Kurihara, T. Kanda, K. Fukai, F. Imazeki, H. Saisho, Distribution of hepatitis B viral genotypes and mutations in the core promoter and precore regions in acute forms of liver disease in patients from Chiba, Japan. Gut 52 (2003) 1630–1637.
[5] T.F. Baumert, S.A. Rogers, K. Hasegawa, T.J. Liang, Two core promoter mutations identified in a hepatitis B virus strain associated with fulminant hepatitis result in enhanced viral replication, J. Clin. Invest. 98 (1996) 2268–2276.
[6] T.F. Baumert, C. Yang, P. Schürmann, J. Köck, C. Ziegler, C. Grüllich, M. Nassal, T.J. Liang, H.E. Blum, F. von Weizsäcker, Hepatitis B virus mutations associated with fulminant hepatitis induce apoptosis in primary Tupaia hepatocytes, Hepatology 41 (2005) 247–256.
[7] I. Pult, T. Chouard, S. Wieland, R. Klemenz, M. Yaniv, H.E. Blum, A hepatitis B virus mutant with a new hepatocyte nuclear factor 1 binding site emerging in transplant-transmitted fulminant hepatitis B, Hepatology 25 (1997) 1507–1515.
[8] T. Kalinina, A. Riu, L. Fischer, H. Will, M. Sterneck, A dominant hepatitis B virus population defective in virus secretion because of several S-gene mutations from a patient with fulminant hepatitis, Hepatology 34 (2001) 385–394.
[9] D. Ganem, A.M. Prince, Hepatitis B virus infection, natural history and clinical consequences, N. Engl. J. Med. 350 (2004) 1118–1129.
[10] N. Liu, L. Ji, M.L. Maguire, D.D. Loeb, Cis-Acting sequences that contribute to the synthesis of relaxed-circular DNA of human hepatitis B virus, J. Virol. 78 (2004) 642–649.
[11] E.B. Lewellyn, D.D. Loeb, Base pairing between cis-acting sequences contributes to template switching during plus-strand DNA synthesis in human hepatitis B virus, J. Virol. 81 (2007) 6207–6215.